Available online at www.sciencedirect.com
SCIENCE DIRECT®
ELSEVIER
Journal of Nuclear Materials 337–339 (2005) 1053–1057
journal of nuclear materials
www.elsevier.com/locate/jnucmat

PSI modeling of liquid lithium divertors for the NSTX tokamak ☆

J.N. Brooks [a,*], J.P. Allain [a], T.D. Rognlien [b], R. Maingi [c]

[a] Argonne National Laboratory, 9700 South Cass Avenue, Argonne, IL 60439, USA
[b] Lawrence Livermore National Laboratory, Livermore, CA 94551, USA
[c] Oak Ridge National Laboratory, Oak Ridge, TN 37831, USA

Abstract

We analyzed plasma surface interaction issues for the planned Module-A static liquid lithium divertor for NSTX using coupled codes/models describing the plasma edge, divertor temperature, and erosion/redeposition, with input data from tokamak and laboratory experiments. A 300 nm lithium pre-shot deposited coating will strongly pump impinging D^+ ions. This yields a low-recycle SOL plasma with high plasma temperature, $T_e \sim 200$–400 eV, low density, $N_e \sim 1$–$3 \times 10^{18}\ m^{-3}$, and peak heat loads of ~8–20 MW/m^2, for 2–4 MW core plasma heating power. This regime has advantages for the NSTX physics mission. Peak surface temperature can be held to an acceptable ⩽470 °C with moderate strike point sweeping (10 cm/s) using a carbon (for 2 MW) or Mo/Cu or W/Cu substrate (2–4 MW). Erosion/redeposition analysis shows acceptable coating lifetime for a 2 s pulse and low core plasma contamination by sputtered lithium.

Keywords: NSTX; Lithium; Erosion/redeposition; Divertor modeling; Density control

1. Introduction

The US advanced liquid plasma surface (ALPS) project is working to develop the science and engineering of liquid metal coated divertors [1]. These systems may help solve the very demanding heat removal, particle removal, and erosion issues of fusion plasma/surface interactions. Liquid lithium divertor experiments are being designed for the National Spherical Torus Experiment (NSTX) at Princeton. A static system ('Module-A') design uses, for every shot, a several thousand Å lithium layer deposited on heated carbon or metal surfaces by pre-shot high yield lithium evaporation [2]. A dynamic system ('Module-B') would use in-shot flowing lithium across the divertor via high speed (~10 m/s) injection. A lithium divertor would aid the NSTX physics mission by strongly pumping D^+, thereby creating a low-recycle high edge temperature plasma regime, with long pulse capability and potential advantages for current drive efficiency and other physics issues.

Key PSI issues are sputter erosion lifetime of the lithium layer, core plasma contamination, and power and particle handling. There is little or no MHD issue with the static system. We use plasma edge/SOL, sputtering, erosion/redeposition, and related codes for this work, following the general plan of [3] with significant model/

☆ Work supported by the US Department of Energy, Office of Fusion Energy.
* Corresponding author. Tel.: +1 630 252 4830; fax: +1 630 252 3250.
E-mail address: brooks@anl.gov (J.N. Brooks).

0022-3115/$ - see front matter © 2004 Elsevier B.V. All rights reserved.
doi:10.1016/j.jnucmat.2004.07.062

data upgrades. The focus here is on the static system – most PSI issues appear to be similar for both systems.

2. NSTX

NSTX is a low aspect ratio spherical torus [4] ($R = 0.86$ m, $a = 0.67$ m, $R/a \geqslant 1.26$, $B_t \leqslant 0.6$ T, $I_p \leqslant 1.5$ MA) with both neutral beam and radio-frequency heating ($P_{NBI} \leqslant 7$ MW, $P_{RF} \leqslant 6$ MW). The goal of NSTX is to determine the attractiveness of the spherical torus concept in the areas of high-β stability, confinement, current drive, and divertor physics, in discharges with quasi-steady conditions for several current diffusion times. Substantial progress [4,5] has been made on the high beta and long pulse performance goals by high energy confinement (H-mode) access which enables high beta limits due to low pressure peaking factors and long pulse operation due to high bootstrap current fraction resulting in volt–second savings.

The longest pulse length exceeds 1 s; these discharges are generally free of edge-localized modes (ELMs) or have very small ELMs. Nearly all of these long discharges have a rapid increase in edge density; given sufficient time (usually 0.3–0.5 s) the core density fills in [5]. This lack of density control limits the ability to perform accurate density scans for physics experiments, and eventually would lead to discharge termination as density limits were exceeded. Thus, a set of tools is being developed for NSTX particle control in 2004–2005, including the Module-A electron beam lithium evaporation system to deposit 100–1000 nm coatings between plasma discharges. The first stage of this deposition could be directly on the existing graphite tiles. However, if the lithium intercalates into the graphite lattice the graphite tiles would be replaced by tiles of a different material (copper, tungsten, or molybdenum), on which a thin chromium layer would be sprayed, followed by a top thin layer of tungsten or molybdenum. The evaporator would deposit lithium on top of this uppermost layer. In this design, the underlying material properties govern the surface thermal response, provided the top thin layers are in good thermal contact with the substrate. We note that the use of a lithium surface to reduce recycling has recently been demonstrated [6] in the CDX-U tokamak. The lithium evaporation system is a first step; a more ambitious flowing liquid lithium, Module-B, has been proposed for integrated density control and heat flux amelioration as part of the long term NSTX plan.

3. Plasma and thermal modeling

The UEDGE-2D plasma fluid code with kinetic corrections [7] is used to compute scrape off layer (SOL) 2-D plasma profiles, from core/edge boundary conditions a few cm inside the magnetic separatrix, and extending to material surfaces where recycling conditions are specified. The kinetic corrections include flux-limiting of parallel thermal conductivity, viscosity, and thermal force, and the low recycling conditions naturally result in nearly uniform electron temperature along each magnetic flux surface. (Although flux limiting is only an approximate procedure, T_e is determined primarily by the power input and the sheath energy transmission for these nearly constant T_e cases.) We model NSTX discharges with 2–4 MW of input power in lower single-null diverted configuration. Fig. 1 shows the SOL geometry and Module-A location (and computed Li density to be discussed). The calculated deuterium plasma background is used as input for the WBC calculation, and then the resulting lithium density at 8 cm above the plate is used as a source in UEDGE to determine the full SOL lithium profile. Particle continuity and parallel momentum equations are solved for each ion charge-state. The inertialess parallel electron momentum equation determines the parallel (along **B**) electric field, in terms of the electron pressure. Separate electron and ion temperature equations are used, with all ion species assumed to have a common temperature. Deuterium neutrals are described by a Navier–Stokes model in the parallel direction and charge-exchange diffusion perpendicular to **B**. Impurity ionization and radiation rates are taken from ADAS. [1]

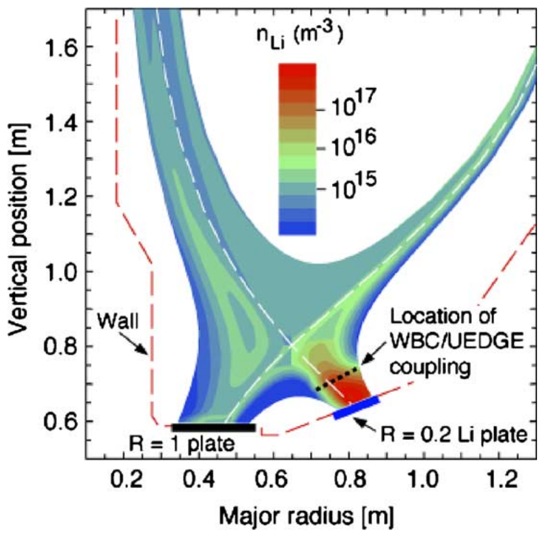

Fig. 1. UEDGE scrapeoff layer geometry, Module-A location, and WBC/UEDGE computed lithium ion density (all charge states) in the SOL for the 2 MW Li/C case.

[1] The originating developer of ADAS is the JET Joint Undertaking.

NSTX Module-A is modeled as having a low ion recycling coefficient, $R = 0.2$, for deuterium ions on the outer (lithium) divertor. (Results were found not sensitive to recycling coefficient in the range $0 < R < 0.5$). The inner divertor is taken to be carbon with unity recycling. The outer wall (carbon) pumps neutrals with an assumed albedo of 0.95.

As a base-case, we take the NSTX EFIT magnetic equilibrium from the single-null discharge 109034. Power into the scrape-off layer is 2, 3, or 4 MW, with an even split between ions and electrons. The ion current across the core boundary is set to 1.0×10^{22} ions/s, which for $R = 0.2$ yields a core boundary density of $3 \times 10^{19}\ \mathrm{m}^{-3}$. ($R = 1$ yields a core density of $5 \times 10^{19}\ \mathrm{m}^{-3}$ with pumping from the wall albedo.) Parallel transport is assumed to be classical. Flux limits are also used for the hydrogen and impurity neutrals, so that any diffusive flux does not exceed the product of the local thermal speed and density. Cross-field transport is assumed to be diffusive owing to plasma turbulence. The anomalous radial transport coefficients are: particles $D = 0.5\ \mathrm{m}^2/\mathrm{s}$, electron and ion energy $\chi_{\mathrm{e,i}} = 1.5\ \mathrm{m}^2/\mathrm{s}$, radial ion viscosity $\eta_{\mathrm{r}} = 1.5\ \mathrm{m}^2/\mathrm{s}$. These values give a reasonable fit to the Thomson scattering edge profiles for discharge 109034, although since we model a low recycling divertor, we assume that these coefficients do not change appreciably. A fixed-fraction of 0.8% carbon is also assumed, which results in a modest amount of carbon line radiation of ~10 kW (rising to 480 kW for the high density $R = 1$ case).

Fig. 2 shows plasma profiles at the outer divertor for the 2 MW case. The low recycling solution has a peak ion density on the inner and outer divertors of $3.0 \times 10^{18}\ \mathrm{m}^{-3}$ and $2.6 \times 10^{18}\ \mathrm{m}^{-3}$, respectively. The corresponding peak electron temperatures are 18 eV and 185 eV, nearly uniform along the flux surface. The radial width of the density and temperature profiles measured at 1/2 the peak is ~4 cm on the outer plate. Peak power flux is 7.9 MW/m^2 on the outer plate, and 4.1 MW/m^2 on the inner plate. The 4 MW case has similar profile shapes with outer plate peak values $T_{\mathrm{e}} = 420$ eV, $N_{\mathrm{e}} = 1.9 \times 10^{18}\ \mathrm{m}^{-3}$, heat flux = 19 MW/m^2.

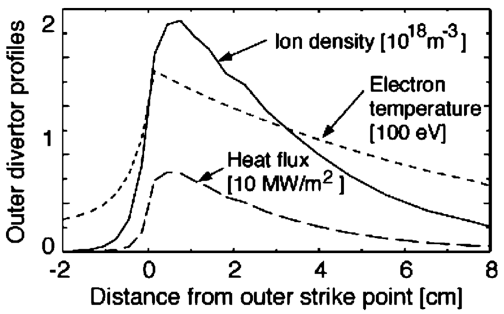

Fig. 2. Plasma solution at the outer divertor for 2 MW plasma heating.

Lithium surface temperature due to the UEDGE-computed heat fluxes is calculated using a time-dependent 1-D semi-infinite slab approximation, both with and without outer strike point sweeping. Initial surface temperature is 200 °C, just above the Li melting point. Temperature-independent heat equation parameters are used corresponding to the substrate. This analysis, while approximate, reasonably defines operating windows in terms of sweep rates, substrate type, plasma power, and pulse length. (Future 3-D, multi-material, full-rigor, thermal analysis, is planned for evolved Module A designs.)

Based on sputter yield increases with temperature and evaporation/sheath-superheat considerations for lithium [8,9], we set a surface temperature limit of 500 °C. This is met – for a full 2 s pulse – for 10 cm/s sweep rate for carbon substrate for 2 MW, and for copper substrate for 2–4 MW. Sweeping of 5 cm/s is also generally feasible. No-sweeping is also possible for Cu – 2 MW, up to 1.4 s. Since sweeping appears to present little or no problems for NSTX, we focus here on 10 cm/s sweep rate cases. Fig. 3 shows surface temperature evolution for the 4 MW Li on Cu case.

We next estimate lithium pumping capacity: For the 2–4 MW solutions the D^+ current to the module is nearly independent of input power, at $\sim 1.0 \times 10^{22}\ \mathrm{D}^+/\mathrm{s}$ – owing to the fixed-flux core boundary condition that will be set by particle fueling in the experiment – giving a maximum $\sim 2.0 \times 10^{22}$ D to be pumped for a 2 s pulse. The peak implanted D^+ distance varies from ~100–200 nm based on VFTRIM runs we made for the energy range of 500–2000 eV D^+ at 45° incidence (with sheath acceleration). Considering also diffusion of the implanted D, the full evaporated layer depth is available for trapping. Using then a roughly 250 nm depth of liquid lithium (to account for some erosion, to be

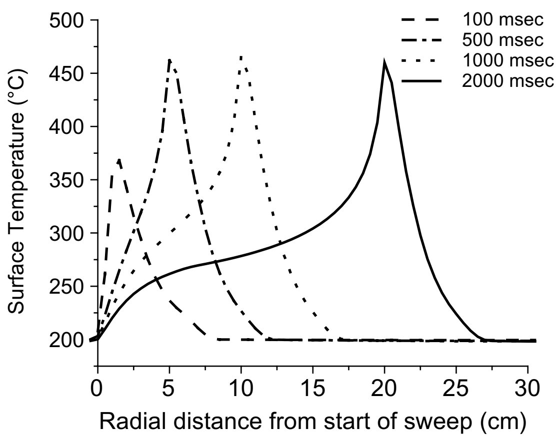

Fig. 3. Temperature profile of thin-film lithium at four discharge times. Copper substrate, 4 MW plasma input power, 10 cm/s sweep rate.

discussed), and a 30 cm swept radial length by 5.4 m toroidal length, the lithium volume available for trapping is $4.1 \times 10^{-7}\ m^3$, which contains $\sim 2.7 \times 10^{22}$ Li atoms. For 1–1 D/Li trapping, e.g., as supported by PISCES data [10] the trapping capacity is 2.7×10^{22} D or about the full D^+ fluence.

Any high capacity pumping system will obviously require significant plasma *refueling*, and this will need to be addressed by NSTX for future operations. We note that some control over D trapping and hence plasma refueling requirements may be obtainable by controlling the Module-A deposited lithium depth.

4. Erosion/redeposition

With inputs of the plasma solutions and time-dependent surface temperature profiles, the REDEP/WBC kinetic Monte Carlo impurity transport code is used to compute sputtering and near-surface transport of lithium. Atoms are launched from the divertor surface per the D^+ flux, temperature-dependent liquid lithium sputter yields, and self-consistent self-sputtering from redeposited lithium ions. Atoms are launched with energy determined from a VFTRIM-verified modified Thompson distribution, for binding energy 1.68 eV. Charge-changing and velocity-changing collisions with the background plasma are computed per detailed kinetic theory. Electron impact ionization of lithium atoms and ions is computed using ADAS database density-dependent rate coefficients. [1] We model the dual ion-gyro-orbit/electrostatic tokamak-type sheath, with total sheath potential $3\,kT_e$. A particle history terminates upon redeposition on the surface, or leaving the $\sim$10 cm wide SOL boundary. A particle that leaves the near-surface region – defined here as 0–15 cm poloidally from the plate – is tracked by UEDGE as mentioned (with a code overlap region of from 8 to 15 cm) and again by WBC for particles re-entering the near-surface region.

Temperature, energy, and angular-dependent lithium sputter yield fits for the WBC analysis were made to data-calibrated VFTRIM-3D runs, for incident D and Li – see [8] for details. We use data from the IIAX facility such data being consistent with recent DIII–D results. The fits use a Sigmund-type temperature-dependent function. Fig. 4 shows fit results for the self-sputter case. Of significance here is that both D and Li yields decrease for high impingement energies calculated for the low-recycle regime.

Li is known to be sputtered mostly (2/3) as Li^+ ions. We treat this effect using a model of immediate redeposition of sputtered ions by the sheath electric field, followed by surface-reflection or sticking of these redeposited ions. Using preliminary molecular dynamics calculations for sputtered/redeposited ion reflection and an estimate of reflected particle charge fraction, this

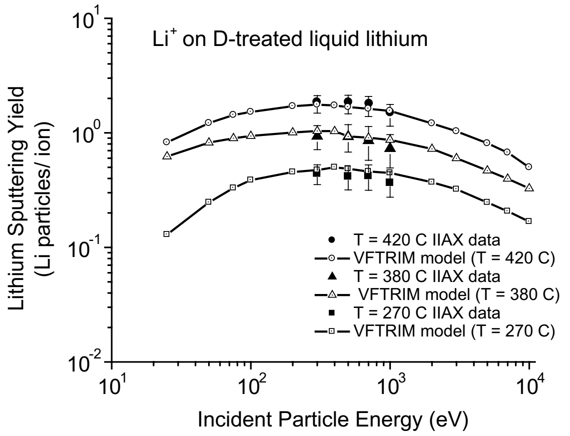

Fig. 4. Lithium self-sputtering yield data (45° incidence) with calibrated simulation output. Temperatures shown include NSTX cases of interest.

model gives the net emitted atom flux $\sim$1/2 total sputtered (atoms + ions) flux.

For each substrate/power combination, the WBC code was run for discrete times in the 0–2 s shot interval, with $\sim 10^5$ histories/run. Key Cu substrate case parameters are listed in Table 1. Other cases are qualitatively similar. In general, redeposition at/near the strike point is low due to long ionization mean free paths in the low density plasma. Lithium tends to be transported from the strike point region to outer radius divertor regions resulting in net growth there. Lithium reaching the 15 cm near-surface boundary varies from about 5–10% of the sputtered current.

For the cases studied about 15–20% of sputtered material leaves the outer SOL boundary. This is not presently further tracked – doing so will require additional modeling of the plasma between the SOL and the first wall. Deposition of some/most of this material

Table 1
Erosion/redeposition summary, Li on Cu-substrate at 1 s

Parameter	2 MW case	4 MW case
Sputtered Li atom mean free path[a]	2.9 cm	4.0 cm
D^+ ion current to module	$1.0 \times 10^{22}\ s^{-1}$	$1.0 \times 10^{22}\ s^{-1}$
Sputtered Li atom current	$1.1 \times 10^{21}\ s^{-1}$	$3.1 \times 10^{21}\ s^{-1}$
Self-sputter fraction	0.13	0.25
D^+ sputter fraction	0.87	0.75
Sputter fraction reaching 15 cm above the plate	0.053	0.087
Sputter fraction to outer SOL boundary	0.17	0.19
Li core contamination fraction, N_{Li}/N_D	$<10^{-4}$	$<10^{-4}$

[a] Perpendicular to surface, average over module.

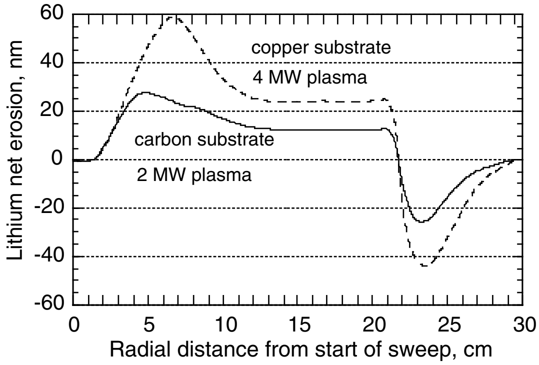

Fig. 5. Module-A lithium net sputter erosion at 2 s end-of-shot. Erosion computed from convolution of swept-plasma net sputter erosion rates for 0–2 s. (Separatrix swept from 2 cm to 22 cm.)

on the first wall adjacent to the outer divertor seems likely. Implications of this, if any, will need assessment.

Fig. 5 shows the time-convolved net erosion after 2 s for the C – 2 MW and Cu – 4 MW cases. Effective peak erosion rates are down by a factor of ~20 from the instantaneous rates, due to the averaging effect of sweeping. Thus the sweeping is of major help. Sweeping of the strike point from outer to inner radius is also a possibility.

Fig. 1 shows the Li ion density in the SOL for the 2 MW Li/C case. Lithium concentration at the outer midplane separatrix is 2.7×10^{-4} of the total electron density, which drops to $\sim 1 \times 10^{-4}$ at the core boundary 2 cm inside the separatrix. The maximum lithium density is $\sim 5 \times 10^{17}\ m^{-3}$, occurring in the near surface region. Thus, the lithium is well confined to the divertor region by friction with the inflowing deuterium and the plate-directed ambipolar electric field. (The Li density very near the plate exceeds 10% of the hydrogen, so that a refined calculation should include this effect by iteration. One result of the Li should be to increase the ambipolar electric field pushing ions back to the plate and thus further reduce the Li upstream.)

5. Other issues

A concern is exposure of high-Z substrate to the plasma if some lithium overlay is lost. This was studied with a WBC analysis of a 1 cm wide toroidally continuous strip of exposed W at the separatrix, but still assuming the low-recycle plasma regime generated by D pumping in the majority Li surface. Results appear encouraging (low W sputtering/contamination in spite of high T_e) but more detailed assessment is needed.

Evaporation of lithium has been studied with detailed sheath/thermal codes [9] showing this as not a significant issue below ~500 °C, but further analysis is needed for conditions peculiar to NSTX, viz. low B field at less oblique angle than most devices. An additional issue is ELM effects on the Li layer which is under study by ALPS personnel (Hassanein et al.).

6. Conclusions

The planned Module-A NSTX thin film deposited liquid lithium system appears to work well from the PSI standpoints assessed. This assumes acceptable thermo/mechanical properties of the deposited Li/substrate system. A lithium on (W, Mo)/copper substrate can handle up to 20 MW/m^2 heat load, using moderate strike point sweeping, sufficient for 4 MW core heating power. Lithium on bare carbon is also an option at lower powers if this should prove feasible from the Li intercalation standpoint. We predict high D pumping by the module for a 2 s pulse. A 300 nm deposited lithium surface is 80–90% retained under sputtering. Core plasma Li sputtering contamination is negligible. A concern is high transport of sputtered material through the lower part of the outer SOL possibly to the adjacent first wall.

The high D pumping by Li yields a low-recycle high temperature plasma regime of major interest in its own right. In general, a lithium divertor for NSTX is seen to be an important application of plasma technology and should provide critical results for future lithium and other liquid metal systems.

Acknowledgments

We thank Dick Majeski (PPPL) for many useful discussions/suggestions, and G.D. Porter (LLNL) for an initial edge-plasma solution.

References

[1] J.N. Brooks et al., Overview of the ALPS program, 16th TOFE, Madison 2004, tbp.
[2] R. Majeski, R. Kaita, R. Maingi, H. Kugel, Pers. Comm., 2003.
[3] J.N. Brooks et al., J. Nucl. Mater. 290–293 (2001) 185.
[4] M. Ono et al., Nucl. Fusion 40 (2000) 557.
[5] R. Maingi et al., Plasma Phys. Control. Fusion 45 (2003) 667.
[6] R. Majeski et al., J. Nucl. Mater. 313–316 (2003) 625.
[7] T.D. Rognlien, M.E. Rensink, Phys. Plasmas 9 (2002) 2120.
[8] J.P. Allain et al., these Proceedings. doi:10.1016/j.jnucmat.2004.10.144.
[9] J.D. Naujoks, J.N. Brooks, J. Nucl. Mater. 290–293 (2001) 1123.
[10] M.J. Baldwin et al., Nucl. Fusion 42 (2002) 131.